Esperamicin A_1 Intercalates into Duplex DNA from the Minor Groove

Norihiro Ikemoto,† R. Ajay Kumar,† Peter C. Dedon,§ Samuel J. Danishefsky,‡ and Dinshaw J. Patel*,†

Cellular Biochemistry and Biophysics Program and Molecular Pharmacology and Experimental Therapeutics Program, Memorial Sloan-Kettering Cancer Center 1275 York Avenue, New York, New York 10021 Division of Toxicology Massachusetts Institute of Technology Cambridge, Massachusetts 02139

Received July 13, 1994

Esperamicin A_1[1] (Figure 1) and calicheamicin γ_1^I[2] are enediyne antibiotics that have generated considerable interest due to their extremely high DNA cleaving potential and associated cytotoxicity.[3] Both drugs possess rather similar aglycones (R) which incorporate novel enediyne functional groups. The drugs undergo reductive cycloaromatization, resulting in the formation of 1,4-diyl species. Direct hydrogen atom transfer from the deoxyribose sugars to the diyls results in oxidative fragmentation of the DNA strand(s). Calicheamicin γ_1^I[4] and esperamicin A_1[5] exhibit distinct sequence specificities for binding and cleavage reactions. Calicheamicin γ_1^I predominantly effects double-strand cuts in the DNA,[4] while esperamicin A_1 causes mostly single-strand breaks.[5] This difference appears to originate from the deoxyfucose–anthranilate moiety (D–E) of esperamicin A_1, which is absent in calicheamicin γ_1^I. Indeed, the product of excission of the D–E sector (esperamicin C) exhibits much enhanced double-stranded cleavage tendencies.[5] In contrast to the calicheamicin γ_1^I–DNA complex, where progress toward a solution structure has been reported,[6] there had been no corresponding structural information with esperamicin A_1. We now report the structure of the esperamicin A_1–DNA complex based on a combined NMR–molecular dynamics study. An important role for the deoxyfucose–anthranilate emerges from this analysis.

The 1:1 complex between esperamicin A_1 and the self-complementary d(C-G-G-A-T-C-C-G) duplex has been prepared[7] and characterized by two-dimensional NMR spectroscopy.[8] A set of distance restraints was obtained between proton pairs from NOESY experiments on the complex recorded in H_2O and D_2O solutions.[9] Restrained molecular dynamics calculations guided by these distance restraints were undertaken from a starting structure using seven different seeds for initial velocity assignments.[10] The seven distance-refined structures of the complex exhibited a pairwise root-mean-square deviation of 1.38 ± 0.20 Å for the central six-base-pair segment centered about the esperamicin A_1 binding site.

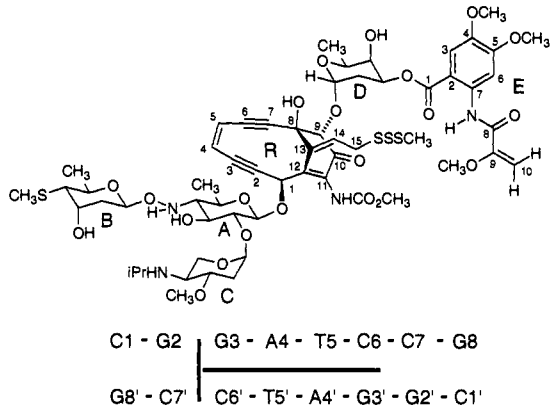

Figure 1. Structure of esperamicin A_1 with the residue designations and numberings. The sequence and numberings of the duplex DNA of the complex are given, and the positions of intercalation and minor groove binding are shown schematically.

A representative distance-refined structure of the esperamicin A_1–d(C-G-G-A-T-C-C-G) duplex complex is shown in Figure 2. Esperamicin binds to the self-complementary octamer duplex through the minor groove, with its methoxyacrylyl–anthranilate group adopting a planar conformation and intercalating into the helix at the (G2-G3)·(C6′-C7′) step.[11] The anthranilate ring stacks over the six-membered rings of G2 and G3 thus providing stability to the complex.[12] The intercalator anthranilate arm is connected to the minor groove binding component via the linker

† Cellular Biochemistry and Biophysics Program, Memorial Sloan-Kettering Cancer Center.

‡ Molecular Pharmacology, and Experimental Therapeutics Program, Memorial Sloan-Kettering Cancer Center.

§ Massachusetts Institute of Technology.

(1) Golik, J.; Clardy, J.; Dubay, G.; Groenewold, G.; Kawaguchi, H.; Konishi, M.; Krishnan, B.; Ohkuma, H.; Saitoh, K.; Doyle, T. W. *J. Am. Chem. Soc.* **1987**, *109*, 3461–3462.

(2) Lee, M. D.; Dunne, T. S.; Chang, C. C.; Ellestad, G. A.; Siegel, M. M.; Morton, G. O.; McGahren, W. J.; Borders, D. B. *J. Am. Chem. Soc.* **1987**, *109*, 3466–3468.

(3) Nicolaou, K. C.; Dai, W.-M. *Angew. Chem., Int. Ed. Engl.* **1991**, *30*, 1387–1416.

(4) (a) Zein, N.; Poncin, M.; Nilakantan, R.; Ellestad, G. A. *Science* **1989**, *244*, 697–699. (b) Dedon, P. C.; Salzberg, A. A.; Xu, J. *Biochemistry* **1993**, *32*, 3617–3622. (c) Li, T.; Zeng, Z.; Estevez, V. A.; Baldenius, K. U.; Nicolaou, K. C.; Joyce, G. F. *J. Am. Chem. Soc.* **1994**, *116*, 3709–3715. (d) Aiyar, J.; Hitchcock, S. A.; Denhart, D.; Liu, K. K. C.; Danishefsky, S. J.; Crothers, D. M. *Angew. Chem., Int. Ed. Engl.* **1994**, *33*, 854–858. (e) Mah, S. C.; Townsend, C. A.; Tullius, T. D. *Biochemistry* **1994**, *33*, 614–621.

(5) (a) Long, B. H.; Golik, J.; Forenza, S.; Ward, B.; Rehfuss, R.; Dabrowiak, J. C.; Catino, J. J.; Musial, S. T.; Brookshire, K. W.; Doyle, T. W. *Proc. Natl. Acad. Sci. U.S.A.* **1989**, *86*, 2–6. (b) Sugiura, Y.; Uesawa, Y.; Takahashi, Y.; Kuwahara, J.; Golik, J.; Doyle, T. W. *Proc. Natl. Acad. Sci. U.S.A.* **1989**, *86*, 7672–7676. (c) Christner, D. F.; Frank, B. L.; Kozarich, J. W.; Stubbe, J.; Golik, J.; Doyle, T. W.; Rosenberg, I. E.; Krishnan, B. *J. Am. Chem. Soc.* **1992**, *114*, 8763–8767.

(6) (a) Walker, S.; Murnick, J.; Kahne, D. *J. Am. Chem. Soc.* **1993**, *115*, 7954–7961. (b) Paloma, L. G.; Smith, J. A.; Chazin, W. J.; Nicolaou, K. C. *J. Am. Chem. Soc.* **1994**, *116*, 3697–3708.

(7) The complex was prepared by stirring 330 λ_{260} units of 8-mer DNA and a fine suspension of esperamicin A_1 (5 mg) in 0.6 mL of NMR buffer for 1 month at pH 7. The final sample was a ca. 3:1 mixture of the 1:1 drug–dsDNA complex and free duplex DNA (see Figure S1).

(8) The NMR data recorded on a Varian Unity Plus 600 MHz spectrometer at 25 °C (NOESY, ROESY, ^{1}H-COSY45, TOCSY, ^{1}H–^{31}P COSY, and ^{1}H–^{13}C COSY) have been fully analyzed and interpreted. Expanded NOESY plots of the base to sugar H1′ proton region along with assignments are plotted in Figure S2.

(9) A total of 359 interproton distances involving nonexchangeable protons were estimated from the D_2O NOE buildups (40, 80, 120, 160, and 200 ms mixing times, 25 °C). Error bounds ranging from ±5% to ±20% of the estimated distances were assigned to the restraints on the basis of the goodness of fit to idealized buildups. In addition, 69 distance restraints involving the exchangeable protons were calculated from the H_2O NOESY spectrum (60 ms mixing time, 5 ° C), for which a uniform error bound of ±20% was used. A total of 44 hydrogen-bonding restraints between base pairs were also imposed. A summary of the distance restraints, which include 88 drug–DNA restraints, is presented in Table S1.

(10) The starting structure was constructed using the parameters for a B-form DNA, and the drug in an extended conformation was placed >6 Å outside the minor groove. The initial model and parameters for esperamicin A_1 were generated using the program QUANTA (v3.3, Molecular Simulations, Inc.) and converted to X-PLOR (Brunger, A. T.) format. A total charge of +1.0 was assigned to the drug because of the protonation of the isopropylamino group of sugar C. The starting structures were subjected to 500 steps of conjugate gradient minimization. Restrained molecular dynamics with simulated annealing was carried out in vacuum with full charges and a distance-dependent dielectic constant using the program X-PLOR. All distance restraints were imposed in the form of square-well potentials. The dynamics was initiated at 5 K, and the temperature was gradually increased to 1000 K in 5.0 ps and then equilibrated for 1.0 ps. The force constants for the distance restraints were kept at 2.0 kcal mol^{-1} Å^{-2} during these stages. Subsequently, the force constants for the distance restraints were scaled up to a final value of 30 kcal mol^{-1} Å^{-2} over 6.0 ps. The system was then allowed to evolve for 10.0 ps at 1000 K before slow cooling to 300 K in 7.0 ps and was then equilibrated for another 10.0 ps. The coordinates saved every 0.5 ps for the last 4.0 ps were averaged, and the resulting structure was minimized. All dynamics were carried out with a time step of 0.5 fs, and the force constant on the Watson–Crick hydrogen bond related distance restraints was maintained at 60.0 kcal mol^{-1} Å^{-2} throughout. The seven distance-refined structures of the complex are plotted in stereo following superposition in Figure S3.

0002-7863/94/1516-9387$04.50/0

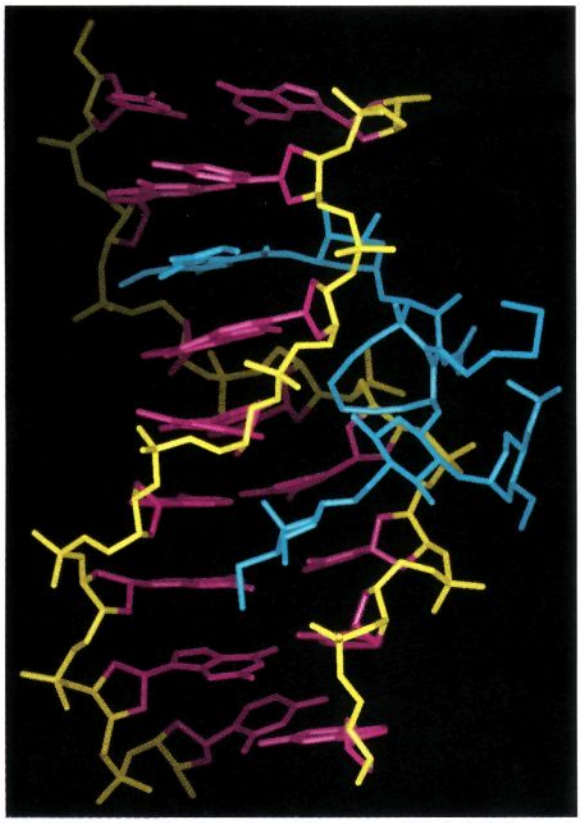

Figure 2. Distance-refined structure of the esperamicin A_1–DNA complex. Esperamicin A_1 is shown in cyan and the DNA in magenta, with the backbone in yellow.

sugar D, whose axial anomeric linkage accommodates a 90° turn at this junction. The enediyne end of R is oriented toward the floor of the minor groove at the A4–T5 step,[13] while the allylic trisulfide trigger is exposed to solvent and is accessible for reductive activation. The A–B–C trisaccharide segment positioned in the minor groove of the esperamicin A_1–DNA complex exhibits features in common with its counterpart in the calicheamicin γ_1^1–DNA complex.[6] Sugar A is positioned face down in the minor groove and lies closer to one strand of the duplex. The hydroxylamino linker orients sugar B perpendicular to sugar A[6] such that it is positioned deep in the center of the minor groove in an edge-on orientation. Sugar C is directed up and over the edge of the minor groove by virtue of its axial linkage to the C^2 position of sugar A, resulting in a favorable electrostatic interaction between its protonated isopropylamino group and the phosphate at the T5-C6 step.

The hydrophobic sugars of esperamicin A_1 provide favorable van der Waals interactions with the hydrophobic walls of the minor groove, and these are favorably positioned by the glycosidic linkages to ideally complement the curvature of the minor groove.[14] The polar groups of esperamicin A_1 also contribute to the sequence specificity and stability through van der Waals interactions, as well as through electrostatic and hydrogen-bonding contributions.[15]

The bound esperamicin A_1 is remarkably well defined in the seven distance-refined structures of the complex and exhibits pairwise root-mean-square deviations of 0.89 ± 0.17 Å.[16] This must reflect the precise anchoring of the enediyne-containing aglycone in the center of the minor groove by the pendent intercalating methoxyacrylyl-anthranilate functionality in one direction and the minor groove-binding A–B–C trisaccharide segment in the opposite direction. The enediyne C^3 atom is 2.6 Å from the C5′ proton (*pro-S*) of C6, identifying the T5-C6 step as the major cleavage site. In addition, the enediyne C^6 atom is directed toward the H1′ (2.7 Å) rather than the H4′ (4.0 Å) proton of the C6′ sugar, accounting for the H1′-mediated abasic site formation opposite single-strand breaks.[17,18]

Our demonstration that the methoxyacrylyl–anthranilate functionality of esperamicin A_1 intercalates at the (G-G)·(C-C) step in duplex DNA is in striking contrast to an earlier molecular dynamics study without experimental restraints which suggested that this functionality resides in the major groove of DNA.[19] Our intercalative structure is supported by independent hydrodynamics and spectroscopic studies on the esperamicin A_1–DNA complex.[17]

Acknowledgment. We thank Dr. T. W. Doyle of Bristol-Myers Squibb for providing a generous sample of esperamicin A_1.

Supplementary Material Available: Tables of distance restraints and intermolecular NOEs, complexation NMR spectra and NOESY plots, stereoview figures of the seven refined structures of the complex and esperamicin A_1, and stacking geometry at the intercalation site (9 pages). This material is contained in many libraries on microfiche, immediately follows this article in the microfilm of the journal, and can be ordered from the ACS; see any current masthead page for ordering information.

(11) The intercalation site is readily identified in the NMR parameters by the absence of sequential intrastrand NOE connectivities between adjacent nucleotides at the G2-G3 and C6′-C7′ steps (Figure S2), the upfield shifts of the imino protons of the intact G2-C7′ and G3-C6′ base pairs, and intermolecular NOEs between the methoxyacrylyl–anthranilate group and these base pairs (Table S2).

(12) The overlap geometry at the intercalation site is shown in Figure S4.

(13) Strong intermolecular NOEs are observed between the H4 and H5 enediyne protons and the imino, H2, and minor groove sugar protons of the A4-T5 step in the complex (Table S2).

(14) The esperamicin A_1 aglycone and sugar B are positioned deep in the minor groove, sugars A and D are aligned along opposite strands of the duplex, and sugar C is positioned over the deoxyribose backbone.

(15) The hydroxyl groups of sugars A, B, and D are positioned close to potential hydrogen bond acceptors represented by the C6-C7 phosphate, the N^3 of A4′, and the O^2 of C7′, respectively. In addition, the carbamate NH of the aglycone is in close proximity to the T5-C6 phosphate.

(16) The best-fit superposition of the seven distance-refined esperamicin A_1 structures of the complex are plotted in stereo in Figure S5.

(17) Yu, L.; Golik, J.; Harrison, R.; Dedon, P. C. *J. Am. Chem. Soc.*, in press.

(18) The prediction of cleavage at C6 and C6′ has been substantiated by sequencing gel analysis of esperamicin A_1-induced damage in 5′-[^{32}P] end-labeled d(CGGATCCG) duplex.

(19) Langley, D. R.; Golik, J.; Krishnan, B.; Doyle, T. W.; Beveridge, D. L. *J. Am. Chem. Soc.* **1994**, *116*, 15–29.